CFD PREDICTION OF RAMJET INTAKE CHARACTERISTICS AT ANGLE OF ATTACK

Soumyajit Saha*, P.K. Sinha* and Debasis Chakraborty*

Abstract

The characteristics of installed intakes of a ramjet engine at angle of attack are predicted numerically. Three dimensional Navier Stokes equations are solved alongwith k - ε turbulence model using commercial CFD software. The software was first validated for isolated intake and computed results match very well with theoretical results available in literature. Pressure recovery Vs. mass flow characteristics of four installed intakes placed in a rear location of a ramjet vehicle is evaluated at different angles of attack upto 6°. Intake performance matches reasonably well with experimental results. It has been observed that significant variation of intake performance exists between windward and leeward intakes. For higher angle of attack, the leeward intake move towards the subcritical operation faster and the intake flowfield is seen to interact with the corebody boundary layer causing significant spillage.

***Keywords**: Air intake, CFD, Pressure recovery, Mass capture*

Symbols

k = turbulent kinetic energy
m = mass captured by the intake
P_0 = total pressure
P_b = intake back pressure
$P_{0\infty}$ = freestream total pressure
m_c = ideal mass capture by the intake
α = angle of attack
ε = turbulent kinetic energy dissipation
π = total pressure recovery
η = mass capture ratio

Introduction

Intake performance is a critical point in the design of ramjet and other supersonic airbreathing mission. The intake of a supersonic airbreathing engine is required to capture and efficiently compress the air so that after heat addition, the flow can be expanded in the nozzle to provide thrust. The design criteria of supersonic air-intake are well documented in the literature [1]. In summary form,

- Intake should provide adequate mass flow of air as demanded by the combustor.
- Intake should compress the flow as efficiently as possible, minimizing the viscous and shock losses. Intake contribution to overall vehicle drag should be kept at minimum.
- Intake performance should not be significantly reduced by operation at incidence.
- Intake must be able to tolerate the back pressure caused by heat addition.
- The velocity profile at intake exit should be as uniform as possible.

Despite its simple geometry, the intake is very sensitive to the interaction with the upstream external flow and downstream combustion process and hence exhibits complex flow phenomena over the expected range of operation. The overall vehicle performance depends greatly on the energy level and flow quality of the incoming air. Small loss in inlet efficiency translates to a substantial penalty in engine thrust. Therefore the detailed analysis and assessment of flow behavior through these components and the interaction with external flow play an important role in the design evaluation and the optimization of the system performance. With the advent of powerful parallel computers and robust numerical algorithm, CFD

* Computational Combustion Dynamics Division, Directorate of Computational Dynamics, Defence Research and Development Laboratory (DRDL), Kanchanbagh Post, Hyderabad-500 058, India, Email : debasis_cfd@drdl.drdo.in
Manuscript received on 11 Feb 2009; Paper reviewed, revised and accepted as a Full Length Contributed Paper on 19 May 2010

is playing an increasing role in the design and analysis of the intake of supersonic airbreathing missions.

Although, many computational studies [2-8] pertaining to various issues of isolated air intake including the unsteady flow [4,5], buzz phenomena [6,7] appeared in the literature, numerical studies for installed air intake are very few. The performance of individual intakes gets modified due to changed entry flow conditions when it is installed to the core body at a downstream location. The variation in performance may be very significant when the vehicle is at angle of incidence.

In this work, numerical simulations are presented for the flow field of installed air intakes mounted on the rear portion of a supersonic ramjet missile using commercial CFD software. The methodology was first validated against the isolated mixed compression air intake result [7] and applied to predict the performance of installed intake for Mach 2 and angle of attack upto 6°. Pressure recovery Vs mass flow characteristics of the intake at various angles of incidence are analysed and compared with the experimental result.

Methodology

Commercial CFD software, CFX TASCflow [9] for isolated intake and CFX-5.7.1 [10] for installed intake are used for the simulation. It solves 3-D Reynolds Averaged Navier Stokes (RANS) equation alongwith k-ε turbulence model on structured grid (CFX TASCflow) /unstructured grid (CFX 5.7.1) based on finite volume approach. The software has four major modules a) *CFX Build*, imports Computer Aided Design (CAD) geometry or creates geometry and generates unstructured volume meshing based on the user input b) *preprocessor* - sets up the boundary condition and initial field condition c) *solver manager* - solves the flow field based on the grid and the boundary condition and d) *postprocessor* - visualizes and extracts the results. In the present computations k-ε turbulence model with scalable wall function at the wall has been used. Local time stepping has been used to obtain steady state solutions.

Validation Study

The flow field of an axisymmetric mixed compression supersonic intake [7] is taken as the case for validation. The schematic of the intake is shown in Fig.1.The front part of the center body involves a double cone with half angles of 20° and 31.25° respectively. The cowl radius is 0.034 m and the throat is located at 0.0787 m from the centerbody nose with a radius of 0.0105 m. The intake configuration was optimum for flight altitude of 9.3 km and Mach No.2.1. The free stream static pressure and static temperature are 0.29 atm and 228K respectively and corresponding total pressure and total temperature are 2.65 atm and 428K. The Reynolds number based on the cowl radius and freestream condition is 0.654 million. The schematic of the computational domain is shown in Fig.2, which contains of both external and internal flow regions. The inclusion of external flow region in computational domain becomes important at subcritical operation when the shock from the center body goes above the cowl lip. Because of the simplicity of the configuration, structured grid is generated and the problem is solved as an axisymmetric one with 3 grid planes in the azimuthal direction. A total of 14,000 finite volume cells are used in the inner domain and 19000 cells are used in the outer domain. The grids are fine near the wall to resolve the boundary layer and relatively coarse in other regions. The computational grid is shown in Fig.3. Freestream supersonic flow is imposed in the inflow boundary and back pressure of 2.1 atm is imposed in the outflow boundary. No slip and adiabatic wall boundary conditions are imposed at the wall. The problem is solved by employing the CFX TASCflow which works on structured data format.

Mach number distribution in the plane of symmetry is compared with the results of Oh et al. [7] in Fig.4. The qualitative agreement between the two simulations is very good. Two leading conical shocks generated at the compression point at the centerbody merge slightly above the cowl lip and form a strong oblique shock extending into the external flow region. The shock emanating from the cowl lip undergoes series of reflection at the centerbody and cowl wall and terminate at the normal shock positioned downstream of the throat. The flow in this region undergoes a series of compression and expansion process; compressed by reflected shock and expanded by the expansion waves. The flow finally becomes subsonic after passing through the normal shock. During the process, the flow direction, which is originally deflected away by the leading shock, is adjusted back to the axial direction. The axial distribution of Mach number and pressure at the centerline of the intake duct is compared with the results of Oh et al. [7] in Fig.5. The wavy distribution of the flow parameters at the centerline demonstrates the complex compression and expansion process in the intake. A good quantitative agreement between the two is obtained although the position of terminal shock for Oh et al. [7] is slightly downstream compared to the present computa-

tions. The difference in the position of terminal shock in the duct may be due to the inadequacy of grid, which could not be resolved in the present study.

Simulation for the Installed Intake

Geometry and Grid Generation

The performance characteristics of an installed intake configuration of a ramjet missile was investigated experimentally [8]. To understand the detailed flow feature inside the intake duct and its interaction with the external freestream flow, numerical simulations are carried out for the same geometry. The schematic of the installed intake configuration is shown in Fig.6. The geometry consists of an ogive-cylinder core body and four integrated air intakes placed in a rear location. The four air intakes are connected to a dump chamber. To avoid the forebody boundary layer, intakes are placed at 1/7 D above the core-body (D is the intake diameter). The air intake has centerbody with semi-cone angle of 27.5°. The intake positioned on the left and right side (seeing from nose) of the pitch plane are marked as east and west respectively whereas the intakes in the windward and leeward position in the pitch plane is marked as south and north intake respectively. The computational domain of the problem is shown in Fig.6 (marked with dotted line), which includes the external flow field of the forebody and the internal flow path in the intakes and the dump chamber. As the interest of the study is to estimate the intake characteristic in installed mode, the external flow domain is terminated at 3 times intake diameter downstream of the cowl lip. Different boundaries are indicated in the figure. Geometry is imported as CAD model and unstructured mesh is generated using CFX 5 software with good clustering near ogive nose, near intake entry. A coarse grid of size 1.1 million and a fine grid of size 3.5 million have been used in the simulation. For fine grid case, points are clustered near the cowl lip region to resolve the flow structure accurately. A typical grid distribution in the pitch plane focusing near the intake entry is shown in Fig.7.

Inflow and Boundary Condition

At inflow boundary (AB and AI), uniform conditions of Mach number, static pressure and static temperature of 2.0, 0.28 atm and 261 K respectively pertaining to wind tunnel condition are imposed. At free stream outlet (BC, CD, GH, HI), supersonic outflow boundary condition is prescribed. At the farthest downstream boundary (EF), exit back pressure is imposed. No slip and adiabatic wall boundary conditions are prescribed at the solid wall. A log normalized rms residue of 1e05 has been set as the convergence criteria.

Results and Discussions

To find out the pressure recovery ($\pi = P_0/P_{0\alpha}$) Vs mass capture ($\eta = m/m_c$) characteristics of the installed intake, simulations were carried out with different angles of attack and back pressure. Starting from 0.8 atm, the back pressure is increased gradually to get the next operating point in the π - η curve. The converged solution of previous back pressure condition is taken as the initial guess for the next simulation, which has accelerated the convergence to a great extent. The qualitative flow features in the intake at zero angle of attack are compared in Figs.8 (a) and (b) for two back pressures of 1.0 and 1.2 atm. The zoomed view near the cowl-lip is also presented in the figure to show that the shock emanating from the centerbody does not touch the cowl-lip and the shock gets detached as the flow deflection angle exceeds the critical angle required for the attached shock at local Mach number. The cowl-lip shock is seen to hit the centerbody and undergoes further reflections. The shock system terminates at the normal shock which is anchored at different downstream position depending on the back pressure. With the increase in the back pressure, the position of the terminal shock is seen to move in upstream location. For back pressure P_b =1.0 atm, the terminal shock is anchored at the end of the intake centerbody and for higher back pressure (P_b =1.2 atm), the terminal shock moved upstream. Mach number distribution in pitch and yaw plane of the air intake at 5° angle of incidence for three different back pressures (p_b =1.2, 1.4 and1.5 atm) are shown in Figs.9, 10 and 11 respectively. For lower back pressure (p_b =1.2 atm) no spillage is seen to occur. Terminal shock for the leeward side intake in the yaw plane has moved upstream compared to the windward side intake; while the flow features of both the intakes at yaw plane remain the same. With the increase in the back pressure, considerable amount of spillage is seen to occur through all the intakes. The leeward side intake in the pitch plane is seen to unstart [Fig.10(a) and Fig.11 (a)]. The terminal shock for the leeward side intake for back pressure P_b =1.5 atm. [Fig. 11(a)] is found to have come out of the intake completely by about one intake diameter. Intakes at the yaw plane is also seen to be affected for higher back pressure. It can be observed from Figs.11 (a) and (b) that the magnitude of the spillage in the yaw plane intakes are much smaller for P_b =1.5 atm compared to the spillage in leeward side intake in the pitch plane. The mass flows through all the intakes at different back pressures at 5° angle of attack are tabu- lated in Table-1. It can be seen

Table-1 : Mass Flow Through Individual Intake at 5° Angle of Attack

Back Pressure (P_b, atm)	Massflow (kg/sec)				
	North (N) Intake	South (S) Intake	East (E) Intake	West (W) Intake	Dump Exit
1.0	0.2536	0.2819	0.2598	0.2594	1.0546
1.2	0.2536	0.2819	0.2598	0.2594	1.0549
1.4	0.1487	0.2742	0.2244	0.2218	0.8690

that mass flow through the East and west intake remain the same while the mass flow through North and south intake are showing difference. At back pressure of 1.4 atm, the mass flow rate through all the intakes showed reduction, minimum mass flow rate is passing through the North intake indicating unstarting of the intake (Fig.10 (a)).

The characteristics of the intakes and the dump plane in terms of pressure recovery Vs the mass flow rate (π - η curve) at zero degree angle of attack is compared with that of experimental value [8] in Fig.12. The computed values of the intake characteristics match reasonably well with the experimental results for the intakes at pitch plane. For zero angle of attack, the characteristics of all the intakes are likely to be same. But in the experimental results it is observed that the characteristics of the windward and leeward intakes in the yaw plane (North and South) are different. The cause is not known. The maximum computed mass flow rate is about 91%.

The intake characteristics for angle of attack 5° have been plotted in Fig.13. It can be seen that the mass capture is never full for the intakes in the supercritical range of operation (the vertical leg of the curve). It can be further seen that the East and West intakes perform similar, while the performance of the North and South intakes vary significantly in subcritical zone. This is due to the difference of flow pattern in the windward and leeward side intakes in the pitch plane for higher back pressure as explained previously while describing the qualitative features of the intake flow field at angle of incidence (Figs.9-11). So the performance of the intakes at angle of attack is significantly different. The π - η characteristics of the intakes and dump plane at 6° angle of attack is compared with the experimental values in Fig.14. A Good overall agreement has been obtained. The computed performance characteristics of the South intake match extremely well with the experimental result; while the computations slightly over-predict the performance of North intake. The performance of North intake deteriorates significantly at higher angle of attack because of its leeward side position. Experimental characteristics of East and West intake show significant difference, whereas the computed characteristics are nearly same. The East and West intakes are placed in yaw plane which is not likely to be affected very much with angle of attack. The difference in the performance observed in the experiment is not very clear. The experimental π - η characteristics at the dump-end located at a distance of 21.6 times the intake diameter from the intake entry is showing a lot of scatter in the data in the supercritical region. An overall good match is obtained between the computation and experimental values.

Conclusions

Numerical simulations are carried out to determine installed air intake characteristics of a ramjet vehicle at angle of attack. Three dimensional Navier Stokes equations are solved alongwith k-ε turbulence model using commercial CFD software. The flow field of an isolated air intake has been taken as a validation case and good qualitative agreement has been obtained for various flow parameters between the computation and other theoretical results available in literature. The pressure recovery Vs. mass flow characteristics (π - η curve) of installed air intakes placed in a rear location of a ramjet vehicle are estimated at different angles of attack upto 6°. The computed π - η characteristics compare reasonably well with the experimental result for different angles of attack. The flow field of the intakes at different angles of attack and at different back pressures were compared to get the insights of the flow behavior of the intake. It was found that the operation regime for the intake in the leeward side in the pitch plane move towards the subcritical regime faster than the other intakes at higher angle of attack and the leeward intake flow field in subcritical mode of operation interacts with the corebody boundary layer and cause significant flow spillage.

Acknowledgement

The authors would like to express their sincere thanks to Dr. B. S. Subhash Chandran, Dr. P. Theerthamalai and Sri Abhishek Richariya, Scientist, Defence Research and Development Laboratory (DRDL) for their help and useful suggestions during the course of the work.

References

1. Seddon, J. and Goldsmith, E.L., "Intake Aerodynamics", AIAA Education Series, 1985.
2. Shigematsu, J. and Yumamoto, K., "Numerical Simulation of Supersonic Inlet Using Implicit TVD scheme", AIAA Paper 90-2135, 1990.
3. Watanabe, Y., Murukami, A. and Fujiwara, H., "Effect of Sidewall Configurations on the Aerodynamics Performance of Supersonic Air Intake", AIAA Paper 2002-3777, 2002.
4. Newsome, R.W., "Numerical Simulation of Near critical and Unsteady Supercritical Inlet Flow", AIAA Journal, Vol. 22, No. 10, 1984, pp. 1375-1379.
5. Fujiwara, H., Murakami, A. and Watanabe, Y., "Numerical Analysis on Shock Oscillation of Two-dimensions External Compression Intakes", AIAA Paper No. 2002-2740, 2002.
6. Lu, P.J. and Jain, L-T., "Numerical Investigation of Inlet Buzz Flow", AIAA Journal, Vol.14, No.1, 1998, pp. 90-100.
7. Oh, J.Y., Fuhara Ma., Shih-Yang Hseih and Vigor Yang., "Interactions Between Shock and Acoustic Waves in a Supersonic Inlet Diffuser", Journal of Propulsion and Power, Vol.21, No.3, pp.486-494.
8. Theerthamalai, P., Mani Sekharan, S., Umakant, J. and Selvarajan, S., "Experimental Investigation of an Installed Air Intake Model", National Conference on Air Breathing Engine 2002, Bangalore, January 2003.
9. User Manual, CFX TASCFlow 2.11.1, AEA Technology, 2001.
10. User Manual, CFX 5.7.1, Ansys India, 2004.

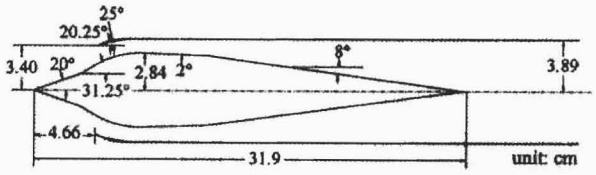

Fig.1 Schematic of the isolated intake geometry

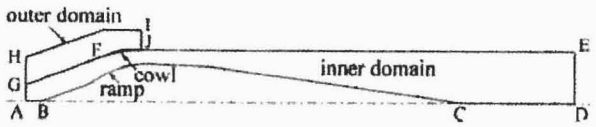

Fig.2 Computational domain showing boundaries

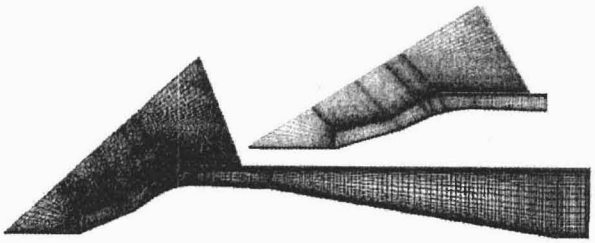

Fig.3 The grid in the computational domain with enlarged view near intake entry

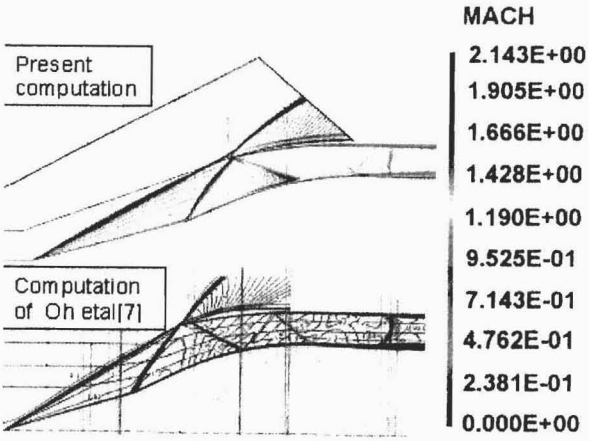

Fig.4 Comparison of computed Mach number contour

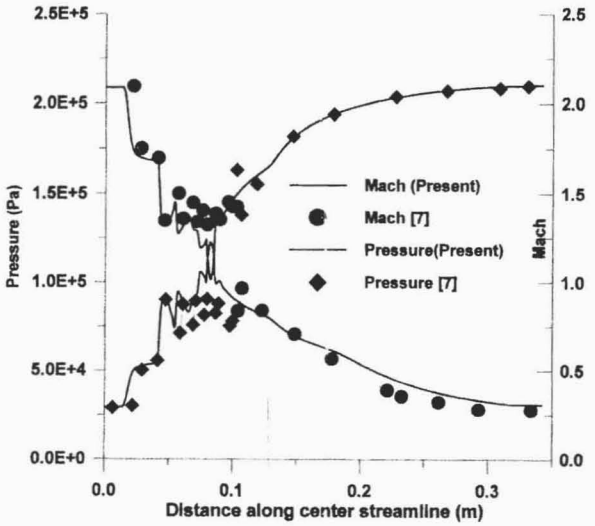

Fig.5 Comparison of pressure and Mach number along central streamline

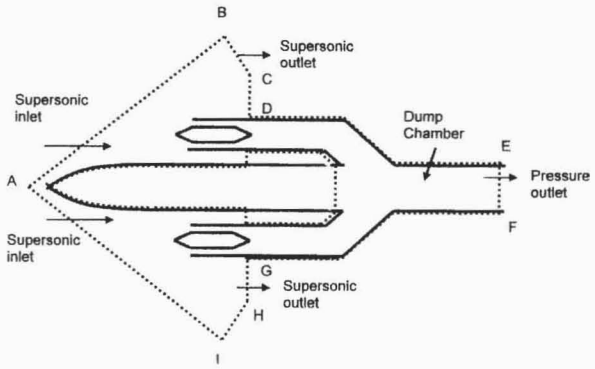

Fig.6 Installed intake geometry and computational domain

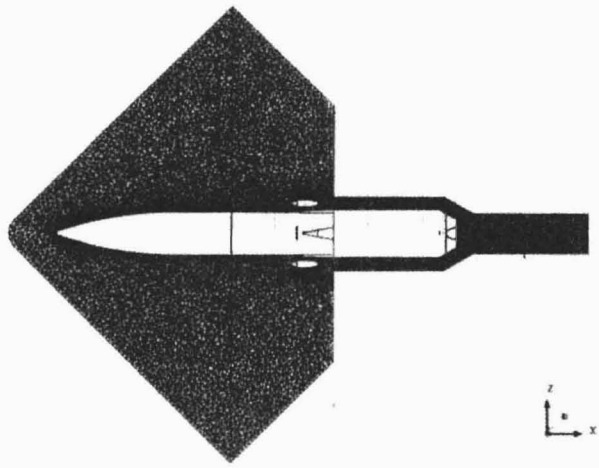

Fig.7 Grid around intake entry

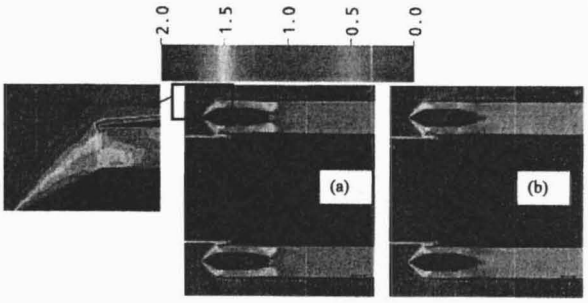

Fig.8 Mach number in pitch plane
(a) P_b = 1.0 atm, (b) P_b = 1.2 atm for AOA - 0°

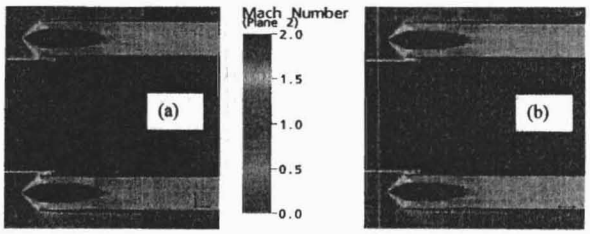

Fig.9 Mach contour in (a) Pitch plane and (b) Yaw plane at P_b = 1.2, AOA = 5°

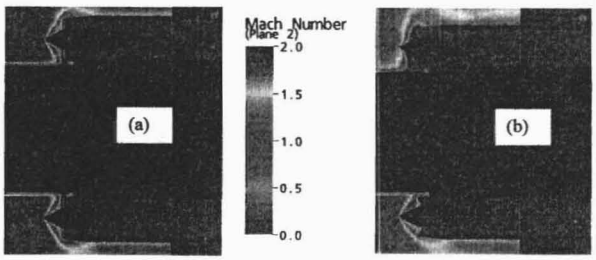

Fig.10 Mach contour in pitch plane at P_b = 1.4 atm, AOA = 5° (a) Pitch plane (b) Yaw plane

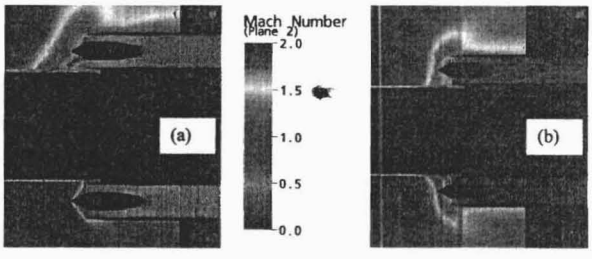

Fig.11 Mach contour in pitch plane at P_b = 1.5 atm, AOA = 5° (a) Pitch plane (b) Yaw plane

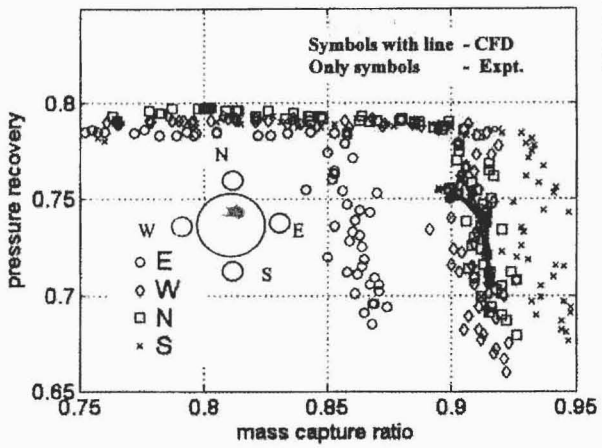

Fig.12 Installed intake characteristics at Mach 2.0 and α = 0°

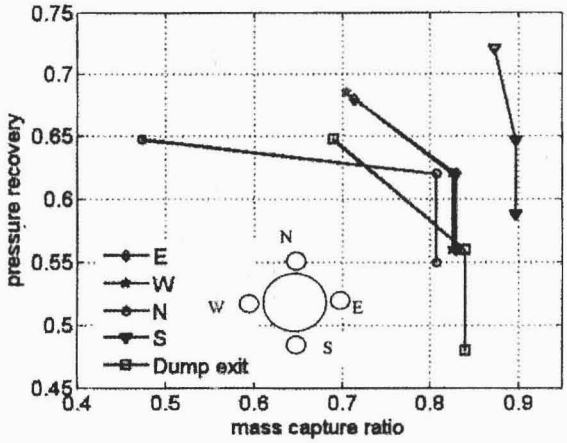

Fig.13 Intake characteristics of different intakes at AOA = 5°

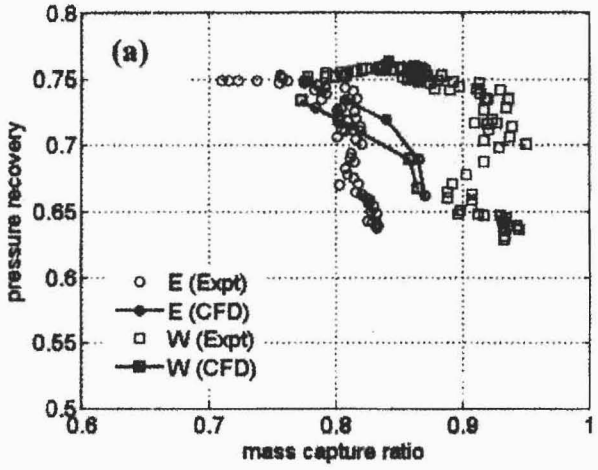

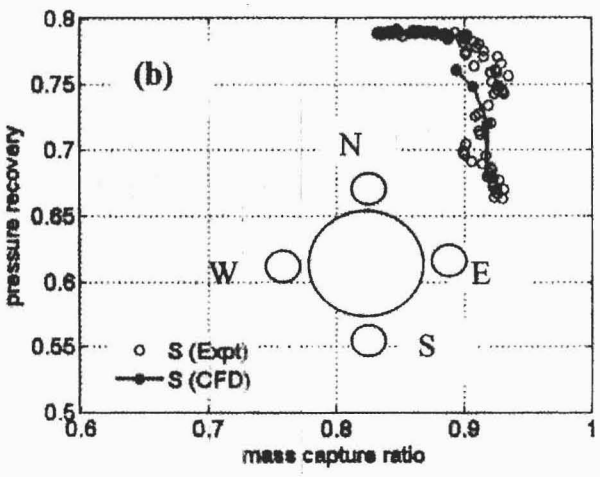

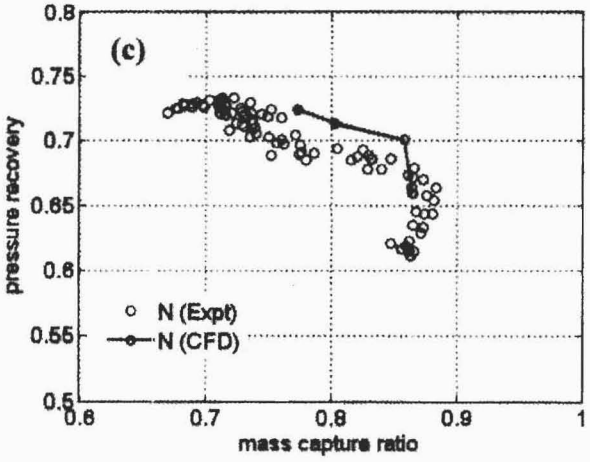

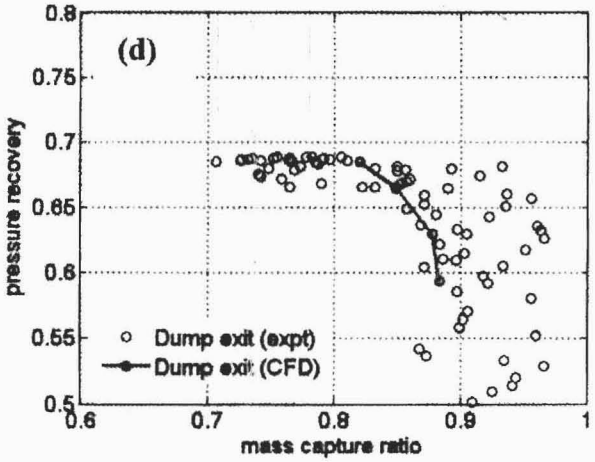

Fig.14 Comparison of installed intake characteristics at Mach = 2.0, α = 6° (a) East and West (b) South (c) North (d) Dump exit